

Variation-based Linearization of Nonlinear Systems Evolving on $SO(3)$ and \mathbb{S}^2

Guofan Wu and Koushil Sreenath

Abstract—In this paper, we propose a variation-based method to linearize the nonlinear dynamics of robotic systems, whose configuration spaces contain the manifolds \mathbb{S}^2 and $SO(3)$, along dynamically-feasible reference trajectories. The proposed variation-based linearization results in an implicitly time-varying linear system, representing the error dynamics, that is globally valid. We illustrate this method through three different systems, a 3D pendulum, a spherical pendulum, and a quadrotor with a suspended load, whose dynamics evolve on $SO(3)$, \mathbb{S}^2 , and $SE(3) \times \mathbb{S}^2$ respectively. We show that for these systems, the resulting time-varying linear system obtained as the linearization about a reference trajectory is controllable for all possible reference trajectories. Finally, a Linear Quadratic Regulator (LQR)-based controller is designed to attenuate the error so as to locally exponentially stabilize tracking of a reference trajectory for the nonlinear system. Several simulation results are provided to validate the effectiveness of this method.

I. INTRODUCTION

Many robotic systems evolve on nonlinear manifolds, such as \mathbb{S}^1 , \mathbb{S}^2 , $SO(2)$, $SO(3)$, $SE(2)$, $SE(3)$. For instance, the configuration space of a spherical pendulum is \mathbb{S}^2 , of a quadrotor is $SE(3) = SO(3) \times \mathbb{R}^3$, and that of a planar n -link robotic snake is $SE(2) \times \mathbb{S}^n$. Moreover, the configuration spaces of multi-link mechanical systems such as the cart with multiple pendulums [15] and humanoid robots are product spaces of \mathbb{S}^2 , $SO(3)$, \mathbb{R}^3 .

Typical dynamical models for studying \mathbb{S}^2 , $SO(3)$ requires setting up local coordinates, such as Euler angles (roll-pitch-yaw), which has the problem of singularity, and thus are not valid globally [27], or global parametrizations that covers the configuration space multiple times, such as quaternions [27], that lead to problems in control such as the unwinding phenomenon [1]. Recent work on *coordinate-free* dynamical models has enabled looking at global, singularity-free, and compact dynamical equations for such systems, enabling design of nonlinear geometric controllers that provide almost-global stability [13], [4], [16], [31], [30].

Although geometric control methods can be used to design almost-global stabilizing controllers, the design is extremely involved, complex, non-intuitive, highly system dependent, and does not lend itself well to embedded implementations. We need a control design method that can track a wide range of dynamically-feasible trajectories in state space, however still

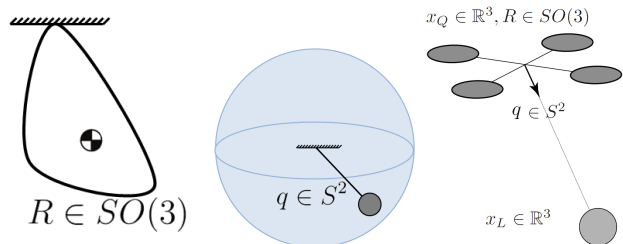


Fig. 1: The 3D pendulum, spherical pendulum, and quadrotor with a cable suspended load are examples of mechanical systems whose dynamics evolve on complex manifolds.

be simple enough to design for an entire class of systems and be easily implementable on these physical systems.

For instance, several nonlinear geometric controllers have been designed for dynamical systems evolving on \mathbb{S}^2 , $SO(3)$, $SE(3)$, $SE(3) \times \mathbb{S}^2$, $\mathbb{R}^3 \times (SO(3) \times \mathbb{S}^2)^n$, and so on; see [16], [12], [31], [17]. These controllers typically implement a PD-type feedback control in the geometric context, where configuration error functions and transport maps are used to compute the position and velocity errors [3]. To deal with model uncertainty, an integral term is added in [12]. These controllers offer almost-global stability properties, where almost any configuration error can be stabilized by the controller. However, designing these type of controllers is extremely dependent on the structure of the dynamical equations of motion, with the design being complex and non-intuitive. Moreover, these controllers might not be easily implemented on physical systems.

In contrast, linear control design techniques are system-independent, with well-established methods, for instance the Linear Quadratic Regulator (LQR). Nonlinear systems have been linearized about reference trajectories to result in locally-valid linear time-varying systems that can then be stabilized to achieve tracking of the reference trajectories, albeit with a smaller domain of attraction. Using results that establish a feedback equivalence between time-varying linear systems and time-invariant linear systems [2], we can also reduce the problem to a linear time-invariant control problem [28]. These linearization methods include Jacobian linearization, feedback linearization, input output linearization, and partial feedback linearization [10], [25], [29].

Powerful as it is in most applications, this type of traditional linearization is problematic when dealing with complex systems that evolve on non-Euclidean manifolds such as $SO(3)$ and \mathbb{S}^2 . Since globally-valid parametrizations do not exist

G. Wu is with the Dept. of Mechanical Engineering, Carnegie Mellon University, Pittsburgh, PA 15213, gwu@cmu.edu.

K. Sreenath is with the Depts. of Mechanical Engineering, Robotics Institute, and Electrical and Computer Engineering, Carnegie Mellon University, Pittsburgh, PA 15213, koushils@cmu.edu.

This work is supported in part by the Google Faculty Research Award and in part by NSF grants IIS-1464337, CMMI-1538869, IIS-1526515.

for these non-flat manifolds, the issue of singularity arises naturally in the linearization process. Employing multiple coordinates would require a highly involved control design that needs to switch between the local charts of these manifolds. Furthermore, as shown in [18], classical linearization is not feedback-invariant under proper coordinate transformation.

Faced with these drawbacks of the traditional Jacobian linearization, recent research has come up with the idea of geometric Jacobian theory [33], [23], [15], [14], [7]. The key idea of this method is to approximate the error on these manifolds by the corresponding variation. Then derive a variation dynamics based on the original system model and utilize it for feedback. For instance, [33] shows a framework of this geometric Jacobian linearization method on a general manifold. Variation-based linearization about a static-equilibrium has been studied in [15], [7], where a chain of pendulum is connected to either a cart, or a quadrotor. In particular, by taking variation about a given static-equilibrium in the state space, a 2nd-order linear time-invariant system (LTI) representing the error dynamics is derived and some discussions about the controllability are given. Similarly, [14] exploits a similar idea to linearize the closed-loop system dynamics with a given geometric control law that closes the loop.

While the previous work is focused on obtaining a time-invariant linearization about a static-equilibrium, we are interested in tracking time-varying reference trajectories. Although some preliminary work along these lines exist [23], [33], the framework provided is abstract, and does not offer a concrete way to analytically determine the variation-based linear dynamics, as well as the controllability of the resulting linear dynamics for any reference trajectory.

The main contributions of this paper with respect to prior work are:

- 1) A variation-based linearization method for linearizing dynamics of systems whose configuration is the product space of \mathbb{S}^2 , $SO(3)$ and \mathbb{R}^n such that the resulting linear model is valid globally, compact, and singularity free.
- 2) Analytical computation of the constraint and the controllable subspaces of the linearized time-varying system *without* requiring explicitly choosing the reference trajectory as a function of time.
- 3) Demonstrating that for systems that evolve on $SO(3)$, \mathbb{S}^2 , \mathbb{R}^n and their product spaces, the resulting families of time-varying linear dynamics are controllable *for all* possible reference trajectories about which the original nonlinear system is linearized.
- 4) A method to design a linear LQR-based controller, that is valid globally and is singularity-free, to track the reference trajectories asymptotically for common robotic systems that evolve on product spaces of $SO(3)$, \mathbb{S}^2 , and \mathbb{R}^n .

The rest of the paper is structured as follows. Section II provides some mathematical preliminaries about variation on \mathbb{S}^2 , $SO(3)$, Section III shows how to get the variation dynamics for a specific system along a reference trajectory

in details, Section IV provides examples for three systems of this type, Section V proposes a linear control design based on the variation dynamics, Section VI presents some simulation results and relevant discussions, Section VII briefly presents some potential applications for robotics, and Section VIII provides some concluding remarks.

II. MATHEMATICAL PRELIMINARY

A. Notation

For a matrix $A \in \mathbb{R}^{n \times m}$, we will use $\mathcal{R}(A)$ and $\mathcal{N}(A)$ to indicate the range and nullspace of A respectively. If A is time-varying, then the respective subspaces are time-varying as well. The symbol I_n is used to represent the identity matrix of size n , and the symbol $0_{n \times m}$ is used to denote a matrix of zeros of size $n \times m$. The hat map $\hat{\cdot} : \mathbb{R}^3 \rightarrow \mathfrak{so}(3)$ is defined by the condition that $\hat{x}y = x \times y$, for all $x, y \in \mathbb{R}^3$, and $\mathfrak{so}(3)$ is the space of skew-symmetric matrices. We will also define the inverse of the hat map, called the vee map, $\vee : \mathfrak{so}(3) \rightarrow \mathbb{R}^3$, such that $\hat{x}^\vee = x, \forall x \in \mathbb{R}^3$. Finally, the exponential map $\exp : \mathfrak{so}(3) \rightarrow SO(3)$ maps a skew-symmetric matrix to a rotation matrix.

B. Linear Time-Varying Systems

A general linear time-varying system is given as

$$\dot{x} = A(t)x + B(t)u,$$

where $x \in \mathbb{R}^n, u \in \mathbb{R}^m, A \in C^\infty(\mathbb{R}^{n \times n})$ and $B \in C^\infty(\mathbb{R}^{m \times n})$. Let's define a linear operator $\mathcal{A}^k = (\frac{d}{dt} + A(t))^k$ (similar to the right operator in [9]) as follows,

$$\begin{aligned} \mathcal{A}^0(B(t)) &:= B(t), \\ \mathcal{A}(B(t)) &:= \frac{d}{dt}B(t) + A(t)B(t), \\ \mathcal{A}^k(B(t)) &:= \mathcal{A}(\mathcal{A}^{k-1}(B(t))). \end{aligned}$$

Then a condition that implies controllability of the above linear time-varying system is, [2],

$$\forall t, \quad \text{rank}(B, \mathcal{A}B, \dots, \mathcal{A}^{n-1}B) = n.$$

C. Variations on Manifolds

To linearize along a reference trajectory on a manifold, we need to take variations with respect to the reference trajectory. We do this through variational vector fields [21], such that the perturbed trajectory is also on the manifold. Here the variation is referred to as *an infinitesimal variation* which could be roughly treated as a linear approximation of the distance between two points on a manifold. For a more formal explanation, we refer to Chapter 5-7 in [20].

By exploiting the specific variation expressions on $SO(3)$ and \mathbb{S}^2 , we are able to parameterize the error directly based on rotation matrices and unit vectors. In this specific error representation, the variation-based linearized dynamics can be derived from the original nonlinear dynamics. We can then design a controller based on the variation-based linearized dynamics which is locally valid on the nonlinear system.

Thus, we will address the following three questions below: what are the error states, what type of constraints should be satisfied on these error states, and finally in order to perform state feedback, how can we design a controller based on the current error state. We will address the first question below, based on [14], and the other questions in the subsequent sections.

1) *Variation in $SO(3)$* : In $SO(3) := \{R \in \mathbb{R}^{3 \times 3} \mid R^T R = I, \det(R) = +1\}$, the infinitesimal variation with respect to a reference $R_d(t) \in SO(3)$ is given by [14],

$$\delta R(t) = \left. \frac{d}{d\epsilon} \right|_{\epsilon=0} R_d \exp(\epsilon \hat{\eta}) = R_d(t) \hat{\eta}(t),$$

where $\eta \in \mathbb{R}^3$. The corresponding infinitesimal change in body angular velocities can be given as:

$$\delta \Omega(t) = \hat{\Omega}_d(t) \eta(t) + \dot{\eta}(t). \quad (1)$$

So if we assume that the actual rotation matrix $R(t)$ is close enough to the desired rotation $R_d(t)$, the state $s = [\eta(t), \delta \Omega(t)]^T$ can be treated as a linear approximation of the errors between the desired and actual state of the system on $SO(3)$. Note that $\eta(t)$ and $\delta \Omega(t)$ are dynamically coupled through the relationship specified in (1).

Given $R(t), R_d(t)$ as the actual and reference trajectory, the actual errors between these two trajectories are given below [3] :

$$\begin{aligned} e_R(t) &= \frac{1}{2}(R_d^T(t)R(t) - R^T(t)R_d(t))^\vee, \\ e_\Omega(t) &= \hat{\Omega}(t) - (R^T(t)R_d(t))\Omega_d(t), \end{aligned}$$

where

$$\Omega(t) = R^T(t)\dot{R}(t), \quad \Omega_d(t) = R_d^T(t)\dot{R}_d(t),$$

and the map $\Omega_d \mapsto R^T R_d \Omega_d$ is called the transport map which allows comparison between tangent vectors at different points. Here we assume that this linear error s is small enough so that they coincide with the actual error. Thus it holds that

$$s = \begin{bmatrix} \eta \\ \delta \Omega \end{bmatrix} \approx \begin{bmatrix} e_R \\ e_\Omega \end{bmatrix} = \begin{bmatrix} \frac{1}{2}(R_d^T(t)R(t) - R^T(t)R_d(t))^\vee \\ \hat{\Omega}(t) - (R^T(t)R_d(t))\Omega_d(t) \end{bmatrix}, \quad (2)$$

which we would use for feedback control on $SO(3)$ in Section V.

2) *Variation in \mathbb{S}^2* : In $\mathbb{S}^2 := \{q \in \mathbb{R}^3 \mid q \cdot q = 1\}$, the infinitesimal variation with respect to a reference $q_d(t) \in \mathbb{S}^2$ is given by [14],

$$\delta q(t) = \left. \frac{d}{d\epsilon} \right|_{\epsilon=0} \exp(\epsilon \hat{\xi}(t)) q_d(t) = \widehat{\xi(t)} q_d(t),$$

where $\xi \in \mathbb{R}^3$, s.t., $\xi \cdot q_d = 0$. The corresponding infinitesimal change in angular velocity is denoted as $\delta \omega(t)$, with the angular velocity defined as $\omega = q \times \dot{q}$.

From [14], the constraints imposed on ξ and $\delta \omega$ can be given below as:

$$\xi \cdot q_d = 0, \quad (\xi \times q_d) \cdot \omega_d + q_d \cdot \delta \omega = 0, \quad (3)$$

The first constraint comes from the variation expression. The second constraint can be derived based on the fact that $\omega \cdot q =$

0. Then the variation of this term $\delta(\omega \cdot q) = \delta \omega \cdot q_d + \omega_d \cdot \delta q = 0$. It follows that $\omega_d \cdot (\xi \times q_d) + q_d \cdot \delta \omega = 0$.

Assuming that the actual direction $q(t)$ is close enough to the desired direction $q_d(t)$ again, the approximated error can be specified as $s = [\xi(t), \delta \omega(t)]^T$ under constraint (3).

For \mathbb{S}^2 , the actual error between $q(t), q_d(t)$ is given as

$$e_q(t) = \widehat{q}_d(t) q(t), \quad e_\omega = \omega(t) - (-\hat{q}^2) \omega_d(t),$$

with $\omega_d \mapsto -\hat{q}^2 \omega_d$ being the transport map.

Applying the same assumption, we would use the following formula for feedback control on \mathbb{S}^2 in Section V:

$$s = \begin{bmatrix} \xi \\ \delta \omega \end{bmatrix} \approx \begin{bmatrix} e_q \\ e_\omega \end{bmatrix} = \begin{bmatrix} \widehat{q}_d(t) q(t) \\ \omega(t) - (-\hat{q}^2) \omega_d(t) \end{bmatrix}. \quad (4)$$

III. SYMBOLIC VARIATION-BASED LINEARIZATION ON PRODUCT SPACE OF \mathbb{S}^2 AND $SO(3)$

Given a system with configuration space $X = X_1 \times X_2 \times \dots \times X_n$ where X_i ($i = 1, 2, \dots, n$) is one of the following three manifolds $\mathbb{R}^3, \mathbb{S}^2, SO(3)$. We list its state variable in three separate groups,

$$\mathbb{R}^3 : (x_1, \dot{x}_1, \dots, x_q, \dot{x}_q) \quad (\text{translational dynamics})$$

$$\mathbb{S}^2 : (q_1, \omega_1, \dots, q_k, \omega_k) \quad (\text{joint dynamics})$$

$$SO(3) : (R_1, \Omega_1, \dots, R_l, \Omega_l) \quad (\text{orientational dynamics})$$

where each $x_i, \dot{x}_i \in \mathbb{R}^3$ represents a rigid body CoM's position and velocity, each $q_i \in \mathbb{S}^2, \omega_i \in \mathbb{R}^3$ reflects the relative position and angular velocity between connecting rigid bodies, and each $R_i \in SO(3), \Omega_i \in \mathbb{R}^3$ are the rotation matrix and body-fixed angular velocity of a single rigid body.

The control input for this system is denoted by $u \in \mathbb{R}^m$. Given a dynamically-feasible reference trajectory $x_d(t)$ with the reference input $u_d(t)$ to follow this trajectory, the following paragraph shows how to derive the variation dynamics around it in a symbolic way.

Assumptions of Variation-based Methods:

- 1) The system dynamics is of 2nd order: This means that the control input u would only appear in the time derivative of $\dot{x}_i, \omega_j, \Omega_p$ where $i \in [1, q], j \in [1, k], p \in [1, l]$.
- 2) The system is control affine with respect to u .
- 3) The dynamic model of the system only consists of vector addition, dot product, cross product and matrix multiplication with a matrix or vector.

According to Assumption (1),(2), the system dynamics could be written out explicitly as:

$$\begin{aligned} \frac{d}{dt} x_i &= \dot{x}_i, & \frac{d}{dt} \dot{x}_i &= f_i + A_i u, & i &= 1, 2, \dots, q, \\ \frac{d}{dt} q_j &= \omega_j \times q_j, & \frac{d}{dt} \omega_j &= g_j + B_j u, & j &= 1, 2, \dots, k, \\ \frac{d}{dt} R_p &= R_p \hat{\Omega}_p, & \frac{d}{dt} \Omega_p &= h_p + C_p u, & p &= 1, 2, \dots, l, \end{aligned}$$

where each $f_i, g_j, h_p \in \mathbb{R}^3, A_i, B_j, C_p \in \mathbb{R}^{3 \times m}$ that are state-dependent vector and matrix functions. Note that the above

assumptions are not restrictive and apply to most mechanical systems, including the 3D pendulum, the spherical pendulum, and the quadrotor with a suspended load that we consider here.

Steps for Generating the Variation-based Linear Dynamics:

- Step 1: We start by taking variation on both sides of the above system dynamics. On the left hand side, we simply add a δ in front of each time-derivative symbol. On the right hand side, we apply the following formulas recursively to get the variation of the functions f_i, g_j, h_p :

$$\begin{aligned}\delta(x + y) &= \delta x + \delta y, \quad \delta(x \times y) = \delta x \times y_d + x_d \times \delta y, \\ \delta(x \cdot y) &= \delta x \cdot y_d + x_d \cdot \delta y, \quad \delta(R_1 x) = \delta R_1 x_d + R_{1d} \delta x, \\ \delta(R_1 R_2) &= \delta R_1 \cdot R_{2d} + R_{1d} \delta R_2,\end{aligned}$$

where $x, y \in \mathbb{R}^3$ and $R_1, R_2 \in \mathbb{R}^{3 \times 3}$, and δ represents the variation. For example, the variation of $\dot{x} = x \times (Ry)$ will result in a variation dynamics as:

$$\begin{aligned}\delta \dot{x} &= \delta(x \times (Ry)) = x_d \times \delta(Ry) + \delta x \times R_d y_d \\ &= x_d \times (\delta R y_d + R_d \delta y) + \delta x \times R_d y_d.\end{aligned}$$

- Step 2: For the control input u , the formulas below are applied to obtain:

$$\begin{aligned}\delta(A_i u) &= \delta A_i u_d + A_{id} \delta u, \quad \delta(B_j u) = \delta B_j u_d + B_{jd} \delta u, \\ \delta(C_p u) &= \delta C_p u_d + C_{pd} \delta u,\end{aligned}$$

where $i \in [1, q]$, $j \in [1, k]$, $p \in [1, l]$, and the variation $\delta A_i, \delta B_j, \delta C_k$ are according to Step 1. Here the variable δu is the control input for which a linear controller will be designed in Section V.

Remark 1: Recall that in Section II we use the symbol δ to represent the 1st order approximation of the actual error on manifold. The formulas presented here are just based on *Chain rule* for matrix-valued functions. Recall that from Taylor's formula, the difference of a function $f: \mathbb{R}^n \rightarrow \mathbb{R}$ has the expression:

$$\begin{aligned}f(x) - f(x_d) &= \nabla f(x_d) \cdot \underbrace{(x - x_d)}_{\delta x} + o(\|x - x_d\|) \\ \implies \delta f &= \nabla f(x_d) \cdot \delta x,\end{aligned}$$

which is exactly the case when the variable is a vector. But here what we consider as variables here could also include matrix.

- Step 3: The resulting variation terms will be in terms of $\eta_j, \delta \Omega_j$ for $SO(3)$, and $\xi_p, \delta \omega_p$ for \mathbb{S}^2 , as shown in Section II. These can be rearranged into a linear system, which forms the variation-based linear dynamics.

Remark 2: It must be noted that this process is carried out symbolically, without specifying an explicit reference trajectory. As we will see, the resulting linear dynamics will be in terms of a symbolic reference trajectory, enabling making conclusions on the controllability properties of the linear system without explicitly choosing a specific reference trajectory.

IV. EXAMPLES OF VARIATION-BASED LINEARIZATION

The method described in the previous section develops the variation-based linearization of a nonlinear system about a reference trajectory. Here we will illustrate the method through three concrete examples: A 3D pendulum, a spherical pendulum, and a quadrotor with a cable-suspended load (see Figure 1). In general, the variation dynamics can be written as the linear system below:

$$\begin{aligned}\dot{s} &= A(x_d(t))s + B(x_d(t))\delta u, \quad (5) \\ C(x_d(t))s &= 0, \quad (6)\end{aligned}$$

where $s = \{\delta x_i, \delta \dot{x}_i, \xi_j, \delta \omega_j, \eta_p, \delta \Omega_p\}$ is the variation for each component introduced in Section III, $\delta u \in \mathbb{R}^m$ is the linear control input, and $C \in \mathbb{R}^{k \times N}$ reflects any constraint that is introduced due to the geometric structure of the manifold.

The linear system produced by the variation-based linearization method represents the linearized dynamics of the errors with respect to the desired reference trajectory about which the nonlinear system was linearized. As can be seen above, the linear system depends on the desired reference trajectory. As we will see, we will design linear controllers for this linearized system to drive the error states $s(t)$ to zero, which in turn will result in tracking the desired reference trajectory for the nonlinear system. However, before we do that, since the system matrices and thus the controllable subspace depend on the desired reference trajectory, we need answer a fundamental question: For what desired trajectories is the variation-based linearization of the nonlinear system controllable? Or, in other words, do there exist desired reference trajectories that render the the above linear time-varying system uncontrollable?

Finally, if there exists constraints, i.e., $C \neq 0$ in (6), then we need to check if state trajectories that respect the constraints are controllable. To do this we introduce the concept of controllability under state constraints.

Definition 1: State-Constrained Controllability: A linear system $\dot{s} = A(t)s + B(t)u$ with state constraints $C(t)s = 0$ is said to be state-constrained controllable, i.e., controllable under the state constraints, if its constraint subspace is invariant and is covered by the controllable subspace.

If a system that is state-constrained controllable as per the definition above, then any state that respects the constraints can be driven to the origin while guaranteeing that the constraint will be feasible for all time. Note that this definition is different to the *constrained controllability* definition in literature, [32], [22], wherein the input (and not the state) is constrained. We will see the above better through the examples below.

A. 3D Pendulum

A 3D pendulum comprises of a rigid body that is attached to a frictionless pivot and subject to gravity. With the state variable $x = (R, \Omega) \in SO(3) \times \mathbb{R}^3$, the system dynamics can be shown as (see [14] for details):

$$\begin{aligned}\dot{R} &= R\hat{\Omega}, \\ J\dot{\Omega} + \Omega \times J\Omega &= -mg\rho \times R^T e_3 + u.\end{aligned}$$

Here $J \in \mathbb{R}^{3 \times 3}$ is the inertia matrix of the pendulum about the pivot, $R \in SO(3)$ the rotation matrix of this body representing its orientation with respect to the inertial frame, g is the scalar gravity constant and $\rho \in \mathbb{R}^3$ the displacement vector from the pendulum's pivot to its center of mass in its body-fixed frame.

Taking variation on both sides about the desired reference trajectory (R_d, Ω_d) , we get the following variation dynamics:

$$\begin{aligned}\delta \dot{R} &= \delta R \hat{\Omega}_d + R_d \delta \hat{\Omega}, \\ J \delta \dot{\Omega} &= -\delta \Omega \times J \Omega_d - \Omega_d \times J \delta \Omega \\ &\quad - mg\rho \times \delta R^T e_3 + \delta u,\end{aligned}$$

Note that since the model here is simple enough, Steps 1,2, of Section II-C are combined together. Using the variation in $SO(3)$ from Section II-C as $\delta R = R_d \hat{\eta}$, $\eta \in \mathbb{R}^3$, and substituting for δR , $\delta \dot{R}$ in the above dynamics, we can simplify the above equation into a linear system below:

$$\begin{aligned}\frac{d}{dt} \begin{bmatrix} \eta \\ \delta \Omega \end{bmatrix} &= \begin{bmatrix} -\hat{\Omega}_d & I_3 \\ -mg\rho \hat{R}_d^T e_3 & J^{-1}(J\hat{\Omega}_d - \hat{\Omega}_d J) \end{bmatrix} \begin{bmatrix} \eta \\ \delta \Omega \end{bmatrix} \\ &\quad + \begin{bmatrix} 0_{3 \times 3} \\ I_3 \end{bmatrix} \delta u,\end{aligned}$$

which is of the form (5)-(6), with A & B obtained from above, with $C = 0$, and the state s as defined in (2).

Remark 3: Note that this is an implicitly time-varying linear system, with the system matrices (A, B, C) only dependent on the desired reference trajectory. As we will see, the system properties, like controllability, and invariant subspaces (with respect to the dynamics) are also dependent on the desired reference trajectory.

We have the following result.

Proposition 1: The linear time-varying system obtained as the linearization of the nonlinear 3D pendulum system about a desired reference trajectory is controllable for all desired trajectories.

Proof: We need to show that $\text{rank} [B \ \mathcal{A}B \ \dots \ \mathcal{A}^{n-1}B] = n$, where the linear operator \mathcal{A} is as defined in Section II-B, and $n = 6$. In particular, we have

$$[B \ \mathcal{A}B] = \begin{bmatrix} 0_{3 \times 3} & I_3 \\ I_3 & J^{-1}(J\hat{\Omega}_d - \hat{\Omega}_d J) \end{bmatrix},$$

which has rank $n = 6$ for all desired trajectories (R_d, Ω_d) , implying that the above system is controllable for all trajectories. ■

Remark 4: It's remarkable that we can analytically verify the controllability of a time-varying system resulting from linearization of a nonlinear system along a trajectory, especially without explicitly specifying the trajectory as a function of time. This is only possible because of the coordinate-free formulation and the variation-based linearization.

B. Spherical Pendulum

A spherical pendulum comprises of a mass attached to a fixed point through a suspended cable. The state of this system

is $x = (q, \omega) \in \mathbb{S}^2 \times \mathbb{R}^3$ with the dynamics:

$$\begin{aligned}\dot{q} &= \omega \times q, \\ ml\dot{\omega} &= q \times (f - mge_3).\end{aligned}$$

Here $q \in \mathbb{S}^2$ is a unit vector that specifies the attitude of the spherical pendulum, $\omega \in \mathbb{R}^3$ is the angular velocity of the spherical pendulum, m is the mass, l is the length, g is the scalar acceleration due to gravity, e_3 is the third directional vector, and f is the controlled force exerted on the spherical pendulum.

Suppose we are given a smooth reference trajectory (q_d, ω_d) to track. Based on Chain rule, taking variation around the reference q_d, ω_d yields the following variation dynamics,

$$\begin{aligned}\delta \dot{q} &= \delta \omega \times q_d + \omega_d \times \delta q, \\ ml\delta \dot{\omega} &= \delta q \times (f_d - mge_3) + q_d \times \delta f.\end{aligned}$$

Substituting for the variation expression $\delta q = \xi \times q_d$, $\xi \in \mathbb{R}^3$, $\xi \cdot q_d = 0$ on \mathbb{S}^2 (from Section II-C), and its time-derivative $\delta \dot{q}$ yields the following error dynamics:

$$\begin{aligned}\frac{d}{dt} \begin{bmatrix} \xi \\ \delta \omega \end{bmatrix} &= \begin{bmatrix} q_d q_d^T \hat{\omega}_d & I_3 - q_d q_d^T \\ (f_d - mge_3) \hat{q}_d / ml & 0_{3 \times 3} \end{bmatrix} \begin{bmatrix} \xi \\ \delta \omega \end{bmatrix} \\ &\quad + \begin{bmatrix} 0_{3 \times 3} \\ \hat{q}_d / ml \end{bmatrix} \delta f,\end{aligned}$$

with the constraint on the states,

$$\begin{bmatrix} q_d^T & 0_{1 \times 3} \\ -\omega_d^T \hat{q}_d & q_d^T \end{bmatrix} \begin{bmatrix} \xi \\ \delta \omega \end{bmatrix} = 0.$$

This is once again of the form (5)-(6), with A, B , and C defined from above and with the state s as defined in (4).

Note that the above system is a constrained linear time-varying system. Traditional analysis would require forming the zero dynamics of this system, as in [9], which is fairly involved. As we will see next, the variation-based linear system obtained by the linearization along a desired reference trajectory is controllable for any reference trajectory that satisfies the constraints.

Proposition 2: The linear-time varying system obtained as the linearization of the nonlinear spherical pendulum system about a desired reference trajectory is *state-constrained controllable*, i.e., it's controllable for all desired trajectories that respect the constraints.

Proof: We will demonstrate this by establishing that the system is state-constrained controllable. We will do this by showing that the constraint space is time invariant, i.e., $\frac{d}{dt}(Cs(t)) \equiv 0$, and that the controllable subspace covers the constraint space, i.e., $\mathcal{R}([B \ \mathcal{A}B \ \dots \ \mathcal{A}^{n-1}B]) \supset \mathcal{N}(C)$. We will do this through the following lemmas. ■

Lemma 1: The constraint space of the variation-based linearized error dynamics of the spherical pendulum is time invariant, i.e., $\frac{d}{dt}(Cs(t)) \equiv 0$.

Proof: We have,

$$\frac{d}{dt}(Cs) = (CA + \dot{C})s + CB\delta u.$$

Here, note that $CB \equiv 0$, since $q_d^T \hat{q}_d \equiv 0$. Moreover,

$$\begin{aligned} (CA + \dot{C})s &= \dot{q}_d^T \xi - q_d^T \delta\omega \\ &= (\omega_d \times q_d) \cdot \xi - q_d^T \delta\omega \\ &= -(-\omega_d^T \hat{q}_d \xi + q_d^T \delta\omega) \\ &= 0, \end{aligned}$$

where the last equality follows from the (second) constraint on the variational linearization of the spherical pendulum. It then follows that $\frac{d}{dt}(Cs) \equiv 0$. ■

Remark 5: From the above lemma, the value $Cs(t)$ is conserved, i.e., if the initial condition satisfies $Cs(t_0) = 0$, then $Cs(t) = Cs(t_0) = 0$, $\forall t \geq t_0$. Thus, as long as the initial condition starts in the constraint space, the system's trajectory is the same as the unconstrained one that evolves according to $\dot{s} = A(x_d(t))s + B(x_d(t))\delta u$. So we could put the constraint aside and treat this system as an unconstrained one.

Lemma 2: The Nullspace of the constraint matrix is given by the column span of the matrix N , and the orthogonal complement of the nullspace of the constraint matrix is given by the column span of N^\perp , where

$$N = \begin{bmatrix} 0 & 0 & \tilde{\omega} & \hat{q}_d \tilde{\omega} \\ \tilde{\omega} & \hat{q}_d \tilde{\omega} & 0 & -q_d \end{bmatrix}, \quad N^\perp = \begin{bmatrix} q_d & \hat{q}_d \tilde{\omega} \\ 0 & q_d \end{bmatrix},$$

where,

$$\tilde{\omega} = \begin{cases} \omega_d, & \omega_d \neq 0, \\ \kappa, \text{ s.t. } q_d^T \kappa = 0, & \omega_d = 0. \end{cases}$$

Proof: We can check that $CN = 0$, $CN^\perp \neq 0$, and $N^T N^\perp = 0$. In these computations, we make use of the fact that $q_d^T \omega_d = 0$. Also note that N is a 6×4 matrix and N^\perp is a 6×2 matrix. In particular, due to the above identities, the columns of N, N^\perp form a full set of basis for \mathbb{R}^6 , i.e., $\text{colspan}([N \ N^\perp]) = \mathbb{R}^6$. ■

Remark 6: It's remarkable that we can analytically write down the nullspace of a time-varying matrix, that resulted from linearization along a trajectory, without specifying the trajectory explicitly as a function of time.

Lemma 3: The controllable subspace of the linearization of the nonlinear spherical pendulum system includes the nullspace of the constraint matrix for all desired trajectories.

Proof: We need to show that $\mathcal{R}([B \ \mathcal{A}B \ \dots \ \mathcal{A}^{n-1}B]) \supset \mathcal{N}(C)$, where the linear operator \mathcal{A} is as defined in Section II-B, $n = 6$, and $\mathcal{N}(C) = \text{colspan}(N)$. We will show that $\mathcal{R}([B \ \mathcal{A}B]) \supset \mathcal{N}(C)$. In particular, we have

$$[B \ \mathcal{A}B] = \begin{bmatrix} 0_{3 \times 3} & -\hat{q}_d/ml \\ -\hat{q}_d/ml & -\hat{\omega}_d q_d/ml \end{bmatrix}.$$

Furthermore, since $\text{colspan}([N \ N^\perp]) = \mathbb{R}^6$, we have $\mathcal{R}([B \ \mathcal{A}B]) = \text{colspan}([B \ \mathcal{A}B][N \ N^\perp])$. By carrying out the matrix multiplication, we can easily show that $\mathcal{R}([B \ \mathcal{A}B]) \supset \mathcal{N}(C)$. In particular, we note that $[B \ \mathcal{A}B]N^\perp = 0$, and $\text{colspan}([B \ \mathcal{A}B]N) \supset \mathcal{N}(C)$. ■

Remark 7: Since the linearized error should always stay within the nullspace of the constraint matrix according to our derivation, results established by the previous lemma guarantee that the origin can be reached from any point that stays in the nullspace, i.e dynamically feasible. Thus the variational linearization of the spherical pendulum is controllable under state-constraints.

C. Single Quadrotor UAV with a Cable-Suspended Load

After applying this technique to two very simple mechanical systems, we now consider a slightly more complicated system that comprises a quadrotor UAV with a cable-suspended pointmass load, analyzed in [31]. The system state is $x = \{x_L, v_L, q, \omega, R_Q, \Omega_Q\} \in \mathbb{R}^6 \times TS^2 \times TSO(3)$ with system dynamics given by [31],

$$\begin{aligned} \dot{x}_L &= v_L, \\ (m_Q + m_L)(\dot{v}_L + g e_3) &= (q \cdot f R e_3 - m_Q l(\dot{q} \cdot \dot{q}))q, \\ \dot{q} &= \omega \times q, \\ m_Q l \dot{\omega} &= -q \times f R e_3, \\ \dot{R} &= R \hat{\Omega}, \\ J_Q \dot{\Omega} + \Omega \times J_Q \Omega &= M. \end{aligned}$$

The variation-based linearized error dynamics can be derived as (see Appendix. A):

$$\begin{aligned} \frac{d}{dt} \begin{bmatrix} \delta x_L \\ \delta v_L \\ \xi \\ \delta \omega \\ \eta \\ \delta \Omega \end{bmatrix} &= \begin{bmatrix} 0 & I_3 & 0 & 0 & 0 & 0 \\ 0 & 0 & A_{23} & A_{24} & A_{25} & 0 \\ 0 & 0 & A_{33} & A_{34} & 0 & 0 \\ 0 & 0 & A_{43} & 0 & A_{45} & 0 \\ 0 & 0 & 0 & 0 & -\hat{\Omega}_d & I_3 \\ 0 & 0 & 0 & 0 & 0 & A_{66} \end{bmatrix} \begin{bmatrix} \delta x_L \\ \delta v_L \\ \xi \\ \delta \omega \\ \eta \\ \delta \Omega \end{bmatrix} \\ &+ \begin{bmatrix} 0 & 0 \\ b_{21} & 0 \\ 0 & 0 \\ b_{41} & 0 \\ 0 & 0 \\ 0 & B_{62} \end{bmatrix} \begin{bmatrix} \delta f \\ \delta M \end{bmatrix}, \end{aligned} \quad (7)$$

with the constraint matrix

$$C = \begin{bmatrix} 0_{1 \times 6} & q_d^T & 0_{1 \times 3} & 0_{1 \times 6} \\ 0_{1 \times 6} & -\omega_d^T \hat{q}_d & q_d^T & 0_{1 \times 6} \end{bmatrix},$$

where each term is defined as,

$$\begin{aligned} A_{23} &= -\frac{1}{m_Q + m_L} [(q_d \cdot f_d R_d e_3 - m_Q L(\dot{q}_d \cdot \dot{q}_d))I_3 \\ &+ f_d q_d (R_d e_3)^T] \hat{q}_d \\ A_{24} &= \frac{2m_Q L}{m_Q + m_L} q_d \hat{q}_d^T \hat{q}_d, \quad A_{25} = -\frac{f_d}{m_L + m_Q} q_d q_d^T R_d \hat{e}_3 \\ A_{33} &= q_d \hat{q}_d^T \hat{\omega}_d, \quad A_{34} = I_3 - q_d q_d^T \\ b_{21} &= \frac{1}{m_L + m_Q} q_d q_d^T R_d e_3, \quad A_{43} = -\frac{f_d}{m_Q L} \widehat{R_d e_3} \hat{q}_d \\ A_{45} &= \frac{f_d}{m_Q L} \hat{q}_d R_d \hat{e}_3, \quad b_{41} = -\hat{q}_d R_d e_3 \\ A_{66} &= J_Q^{-1} (\widehat{J_Q \Omega_d} - \hat{\Omega}_d J_Q), \quad B_{62} = J_Q^{-1}. \end{aligned}$$

Proving the constrained controllability of this system using direct method is intractable since we need to take higher order time-derivatives for both A and B .

V. LINEAR CONTROLLER DESIGN FOR VARIATION-BASED LINEARIZED SYSTEM

Having presented the variation-based linearization dynamics for three different example systems evolving on $SO(3)$, \mathbb{S}^2 , and $SE(3) \times \mathbb{S}^2$ respectively, we will now develop a LQR-based controller to track desired reference trajectories for these nonlinear systems. Recall that from results in classical control, controllers designed on the linearized model guarantee local exponential stability when applied on the original nonlinear system. Since the variation-based linearization is a linear approximation of the nonlinear system, linear controllers designed using the linear time-varying system work on the nonlinear system with large domains of attraction.

Since the variation-based linearization system is a time-varying system, we propose designing a time-varying LQR controller. We must note that for the spherical pendulum and the quadrotor with suspended load systems, the linearized system is subject to state constraints, i.e., some entries in s depend implicitly on other states. To address this, one would need to design the LQR controller on a reduced system that has an independent set of unconstrained states. However, as we have seen in the previous section, these constraints are time-invariant, and the controllable subspace covers the constraint subspace. We can thus carry out the LQR control design directly on the constrained system, with the requirement that initial condition starts in the constraint subspace.

Finite-Horizon Linear Quadratic Regulator Design:

We design a time-varying LQR controller for the variation-based linearized dynamics. We begin with a desired dynamically feasible reference trajectory, x_d , and a nominal control input, u_d , that achieves the reference motion. The nonlinear system that evolves on manifolds is linearized along this trajectory using the variation-based linearization method presented in the prior sections to obtain a time-varying linear system. A finite horizon LQR controller design is carried out on this time-varying system. Figure 2 illustrates a block diagram of the control.

We begin with the state $s(t)$ of the variation-based linearized system. This state represents the linearized geometric error and can be computed using the formulas (2) and (4) in Section II. We choose a time horizon T and pick matrices $Q_1 = Q_1^T \geq 0 \in \mathbb{R}^{n \times n}$, $Q_2 = Q_2^T > 0 \in \mathbb{R}^{m \times m}$ as the weights on the states $s(t)$, and the controls $\delta u(t)$. Here n represents the dimensions of the states and m the dimensions of the inputs. We also choose $P_T = P_T^T \geq 0 \in \mathbb{R}^{n \times n}$ as the weight on the terminal state $s(T)$.

Next, the continuous-time Riccati equation below is integrated backwards in the time,

$$-\dot{P}(t) = Q_1 - P(t)B(t)Q_2^{-1}B(t)^T P(t) + A(t)^T P(t) + P(t)A(t),$$

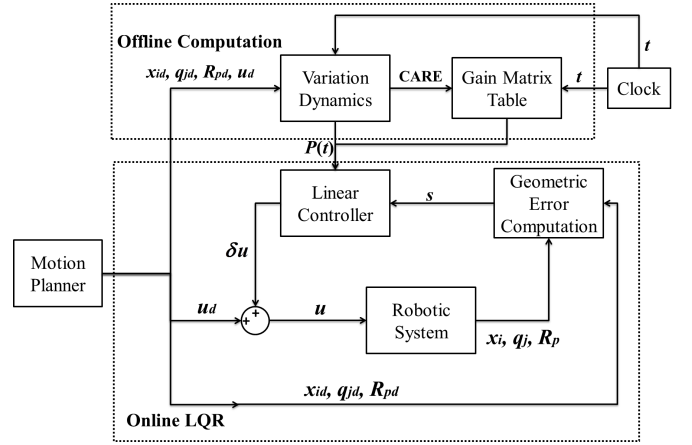


Fig. 2: Block diagram representing the time-varying LQR controller, designed on the variation-based linearized system, and applied to the original nonlinear system evolving on manifolds.

starting from the terminal condition $P(T) = P_T$. The control applied to the nonlinear system is computed as,

$$u(t) = u_d(t) + K(t)s(t),$$

where the gain matrix $K(t) = -Q_2^{-1}B(t)^T P(t)$.

Remark 8: Note that once the proposed variation-based linearization is carried out on the nonlinear system evolving on manifolds, the resulting linearized dynamics is essentially a linear time-varying system, and standard control design techniques from linear control theory can be carried out. In particular, the linear quadratic regulator (LQR) is an optimal control technique applicable to linear time-varying systems [19]. The corresponding feedback gain for the LQR is the solution of the continuous Riccati equation, and it only depends on the linearized dynamics (which depend on the reference trajectory), the weighting matrices and the time horizon. Thus, once we fix a specific reference trajectory, the corresponding LQR gain matrix can be computed offline and stored in a lookup-table.

Remark 9: We employ a finite-horizon LQR controller here since in most robotic applications a motion planner only produces a finite-horizon reference trajectory. Alternatively, an infinite-horizon LQR can also be implemented, assuming we have the complete reference trajectory and the linearized dynamics is controllable (we have explicitly shown controllability of the variation-based linearized 3D and spherical pendulum systems for all possible reference trajectories.)

As we will see in the next section, since the linear control design is carried out on the variation-based linearization, it's free of singularities. Moreover, this method also admits a potentially large domain of attraction. We will demonstrate these features on all three examples considered in this paper - the 3D pendulum, the spherical pendulum, and a quadrotor with a cable-suspended load.

VI. SIMULATION RESULTS

We use the variation-based linearization and controllers presented in the previous sections to perform several simulations to test the effectiveness of our proposed method. Additional results are also provided for comparison to show the robustness of this method. An interesting fact about all the systems studied here is that all of them are *differentially flat*, [6], wherein knowing the time-varying trajectory of a set of flat outputs enables us to analytically compute the time trajectories of the entire state as well as the control input that results in this state trajectory through higher order time derivatives of the flat output. This enables planning dynamically-feasible reference trajectories very easily. It must be noted that the flat outputs need not be just a subset of the states, but rather can be a function of the states, the inputs, and higher order time derivatives of the inputs. We now present simulation results for these three systems presented in the paper.

A. 3D Pendulum

The rotation matrix, R_d , corresponding to the rigid body orientation, forms a set of flat outputs for this system since the angular velocity can be computed from \dot{R}_d and the control can be computed from the time derivative of the angular velocity and the system parameters. We use the system parameters $l = 1$, $\rho = 0.5e_3$, $J = \text{diag}(0.1006, 0.1006, 0.0127)$, $m = 0.2827$, and chose the flat output as,

$$R_d(t) = \begin{bmatrix} \cos \omega_0 t & \sin \omega_0 t & 0 \\ -\sin \omega_0 t & \cos \omega_0 t & 0 \\ 0 & 0 & 1 \end{bmatrix}, \quad \omega_0 = 1.5.$$

The following matrices were used to design the LQR controller, $Q_1 = \text{diag}(2, 2, 2, 5, 5, 5)$, $Q_2 = 0.5I_3$, $P_T = 2.5I_6$. The initial condition for simulation is specified as

$$R_0 = \text{diag}(1, -1, -1), \quad \Omega_0 = [-1.5, 0.8, 1.0]^T.$$

This corresponds to a maximum possible error in orientation. As we will see, the linear controller has a large domain of attraction. Figure 3 shows the simulation results for the 3D pendulum, illustrating tracking of the reference trajectory. The errors e_R, e_Ω in the figure are errors on $SO(3)$, computed as, [16],

$$e_R = \frac{1}{2}(R_d^T R - R^T R_d)^\vee, \quad e_\Omega = \Omega - R^T R_d \Omega_d.$$

The configuration error is computed as,

$$\Psi_R = \text{trace}(I - R_d^T R)/2,$$

with $\Psi_R = 0$ when $R = R_d$, and $\Psi_R = 2$ when there is a 180° error between R and R_d . As can be seen from the figure, the controller is able to stabilize large initial errors in attitude. Here we demonstrate the controller recovering from the largest possible attitude error with $\Psi_R = 2$. However, we must note that although the linear controller results in exponential stability on the nonlinear system for small (local) errors, the controller only results in asymptotic stability for large (global) errors. This is evident in the plot of the configuration error

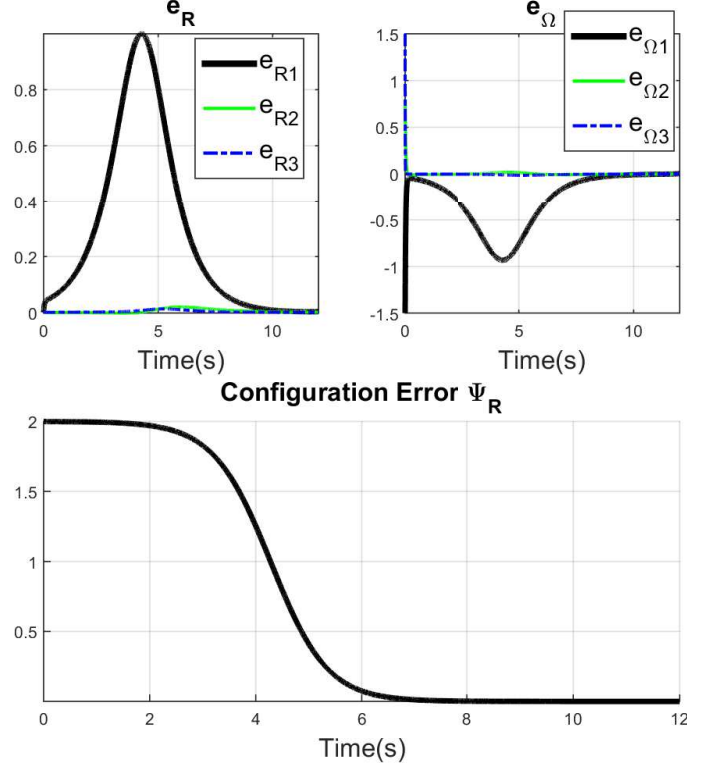


Fig. 3: Tracking errors obtained by simulating the variation-based linearization controller for the 3D pendulum system described in Section VI-A. In particular, the vector error function for the position and velocities, e_R , e_Ω , and the configuration error function, Ψ_R , are shown as functions of time. Here we set the initial configuration error $\Psi_R = 2$, the maximum possible orientation error, and the linear controller is still able to asymptotically track the reference trajectory.

Ψ_R in Figure 3. Further, note that the initial configuration error $\Psi_R = 2$ corresponds to one of the equilibrium points for the open-loop 3D pendulum with $e_R = 0$. The controller is able to recover from this initial error, albeit slowly, due to the feedforward component of the control.

B. Spherical Pendulum

As mentioned in Section IV-B, the spherical pendulum system we are considering consists of a mass attached to a fixed point through a suspended cable. It turns out that the flat output for this system is the tension force vector in the cable. This flat output is a function of both the state and the control input on the system. The tension vector is a flat output since the cable orientation specified by $q_d \in S^2$ can be obtained from the tension vector, the angular velocity can be obtained from q_d and its time-derivative, and finally the control input can be obtained from the time-derivative of the angular velocity and the system properties. We specify the following flat output to generate the reference trajectory for

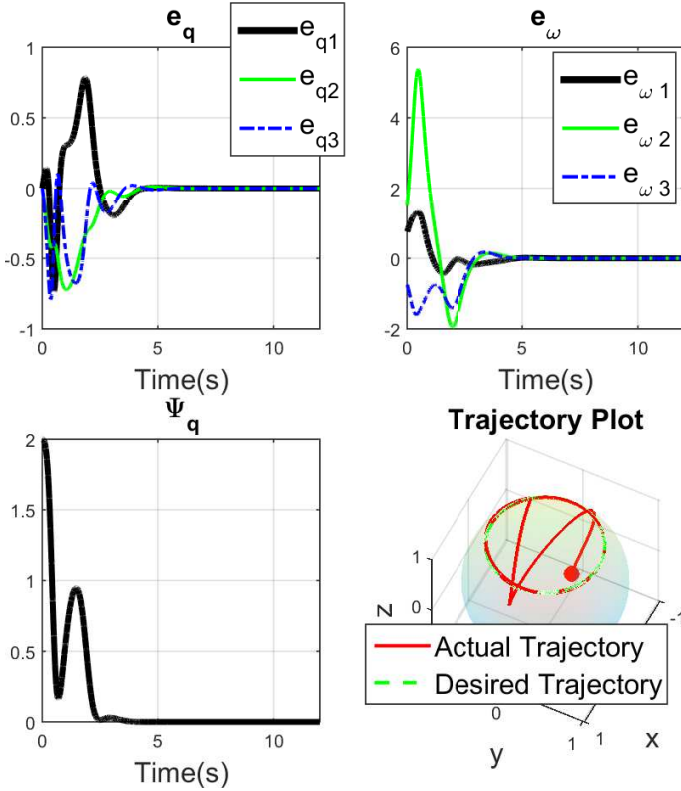


Fig. 4: Tracking errors obtained by simulating the variation-based linearization controller for the spherical pendulum system, as described in Section VI-B, is shown. In particular, the vector error function for the position and velocities, e_q , e_ω , and the configuration error function, Ψ_q , are shown as functions of time. In addition, the desired trajectory is shown on the unit sphere with the actual trajectory tracking the desired.

tracking:

$$T_d(t) = 5[\cos \frac{\pi}{6} \cos 1.5t, \cos \frac{\pi}{6} \sin 1.5t, \sin \frac{\pi}{6}]^T,$$

with the initial conditions $q_0 = [-\sqrt{2}/2, 0, -\sqrt{2}/2]^T$, $\omega_0 = [0, 1.5, 0]^T$. For the simulation, we select the following gain matrices are used, $Q_1 = \text{diag}(50, 50, 50, 15, 15, 15)$, $Q_2 = 0.25I_3$ and $P = I_6$. The error functions e_q, e_ω, Ψ_q are errors on \mathbb{S}^2 , computed as, [17],

$$e_q = \hat{q}_d q, \quad e_\omega = \omega - (-\hat{q}^2)\omega_d, \quad \Psi_q = 1 - q \cdot q_d.$$

Fig. 4 shows relevant tracking results of the LQR controller designed on the variation-based linearization and applied to the spherical pendulum system. As can be seen from the figure, stability can be guaranteed using our method even for the cases with very large initial error.

C. Single Quadrotor UAV with a Cable-Suspended Load

This quadrotor with a cable-suspended load system is also differentially flat, with the load position x_L and quadrotor yaw ϕ as flat outputs, see [31] for more details. We thus specify

TABLE I: Initial Conditions for Simulation

| Initial State | Trial 1 | Trial 2 | Trial 3 |
|---------------|--------------------------|---------------------------|--|
| x_{L0} | $[0, 5, -1.5]^T$ | $[0, 0, 0]^T$ | $[-1, 0, 1]^T$ |
| v_{L0} | $[0, 0, 0]^T$ | $[0, -1, -1]^T$ | $[0, 0, 0]^T$ |
| q_0 | $[0, 0, -1]^T$ | $[0; \sqrt{3}/2, -0.5]^T$ | $[\sqrt{2}/4, \sqrt{6}/4, \sqrt{2}/2]^T$ |
| ω_0 | $[0, 0, 0]^T$ | $[-0.5, 0, 0]^T$ | $[0, 0, 0]^T$ |
| R_{Q0} | $\text{diag}(1, -1, -1)$ | I_3 | I_3 |
| Ω_{Q0} | $[0, 0, 0]^T$ | $[1.5, 0, 1]^T$ | $[0, 0, 0]^T$ |

the following flat output to generate the reference trajectory and nominal input,

$$x_{Ld}(t) = [\cos t, \sin t, 0.5t]^T, \quad \phi_d(t) \equiv 0.$$

For the LQR control design, the weighing matrices are set as

$$Q_1 = \begin{bmatrix} Q_{11} & 0 & 0 \\ 0 & Q_{22} & 0 \\ 0 & 0 & Q_{33} \end{bmatrix}, \quad \text{where,}$$

$$Q_{11} = 0.5 \cdot I_6, \quad Q_{22} = I_3, \quad Q_{33} = 0.75I_9, \\ Q_2 = 0.2I_4, \quad P_T = 0.01 \cdot I_{18}.$$

We evaluate the performance of the controller in three trials by specifying different initial conditions for the 18-dimensional state, as tabulated in Table. I. Figure 5 illustrates the convergence to the reference trajectory starting at the three initial conditions. Note that, for trial 1, the quadrotor is initially inverted, and the controller is still able to track the specified reference trajectory, illustrating that the linear controller has a large domain of attraction. Figure 6 depicts the tracking performance of the controller for the three initial conditions. As can be seen, in all the cases, the translational error in the quadrotor position, and the rotational errors for both the quadrotor orientation and the cable attitude go to zero. This illustrates the validity of the proposed method for higher-dimensional systems and demonstrates the large domain of attraction that is possible through a linear controller.

D. Robustness Test on the Quadrotor-Load System

The stability properties of the linear control design based on the variation-based linearization have been shown in the previous simulation examples. We next test the robustness of the proposed method by subjecting the controller to model uncertainty by varying the mass of the load. Fig. 7 illustrates the effects of increasing the mass of the load by 50% and decreasing the mass by 10%. In both cases, we test the controller for the same initial conditions considered in Trials I-III in Table I. As can be seen, this method is robust to the considered model uncertainties since it keeps the error bounded. The robustness can potentially be further improved by applying linear robust control techniques, [8], designed

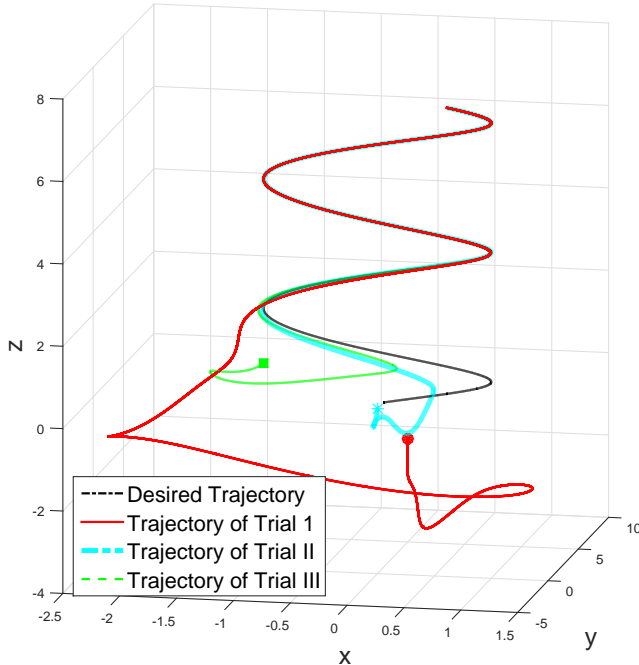


Fig. 5: Load trajectory plot obtained by simulating the variation-based linearization controller for the quadrotor with a cable suspended load, as described in Section VI-C, for the three initial conditions is shown. The initial conditions are denoted by bold points in the figure. For each initial condition, the variation-based linearization controller is able to drive the load to the desired trajectory.

on the variation-based linearized system and applied to the nonlinear system.

VII. POTENTIAL ROBOTIC APPLICATIONS

The proposed method of variation-based linearization has several potential applications in robotics, such as motion planning, filtering, and control [5], [26], [24], [11]. As presented in this paper, this method can be used to implement linear controllers for systems that vary on manifolds while preserving the global validness, singularity-free, and compact properties of the linear model. Furthermore, this method can also be used for deriving linear time-varying models of robotic systems for the purpose of estimation through extended Kalman filters (EKF) directly on the \mathbb{S}^2 and $SO(3)$ manifolds, see [24].

VIII. CONCLUSIONS

This paper has presented a variation-based method to linearize a nonlinear system, whose dynamics evolve on complex manifolds that contain $SO(3)$ and \mathbb{S}^2 , along a desired reference trajectory. The resulting linear system is implicitly time varying. Three example systems, the 3D pendulum, spherical pendulum and a quadrotor with a suspended load, are studied, and the corresponding linearized error dynamics about a reference trajectory are developed. For the first two examples,

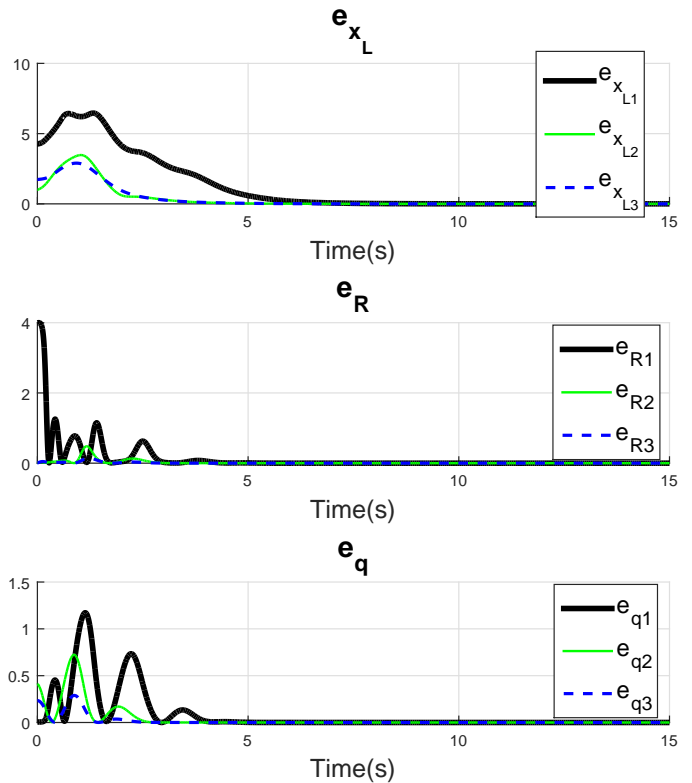


Fig. 6: Tracking errors obtained by simulating the variation-based controller for the quadrotor with a cable suspended load, as described in Section VI-C, for the initial condition specified by Trial III is shown. In particular, the translational position errors, e_{x_L} , and vector errors for the quadrotor orientation, e_R , and load orientation, e_q , are shown as functions of time.

we show that the families of time-varying linearizations are controllable for all possible desired trajectories. Finally, a time-varying LQR controller is developed and several trajectory tracking results for the nonlinear systems are shown. Simulation tests indicate that the regions of attraction of these controllers are fairly large.

APPENDIX

A. Error Dynamics Derivation for the Quadrotor with a Suspended Load

In Sections IV-A, IV-B, we derived the variation-based linearization of the 3D and spherical pendulums respectively. Here we provide a detailed derivation of the variation-based linearization of the quadrotor with a cable-suspended load system about a desired reference trajectory. First, symbolically taking the variation of the dynamics of the quadrotor with a cable-suspended load, specified in (IV-C), yields,

$$\begin{aligned} \delta \dot{x}_L &= \delta v_L, \\ (m_Q + m_L) \delta \dot{v}_L &= [\delta q \cdot f_d R_d e_3 + q_d \cdot (\delta f R_d e_3 + f_d \delta R e_3) \\ &\quad - 2m_Q L (\dot{q}_d \cdot \delta \dot{q})] q_d \\ &\quad + (q_d \cdot f_d R_d e_3 - m_Q L (\dot{q}_d \cdot \dot{q}_d)) \delta q, \end{aligned}$$

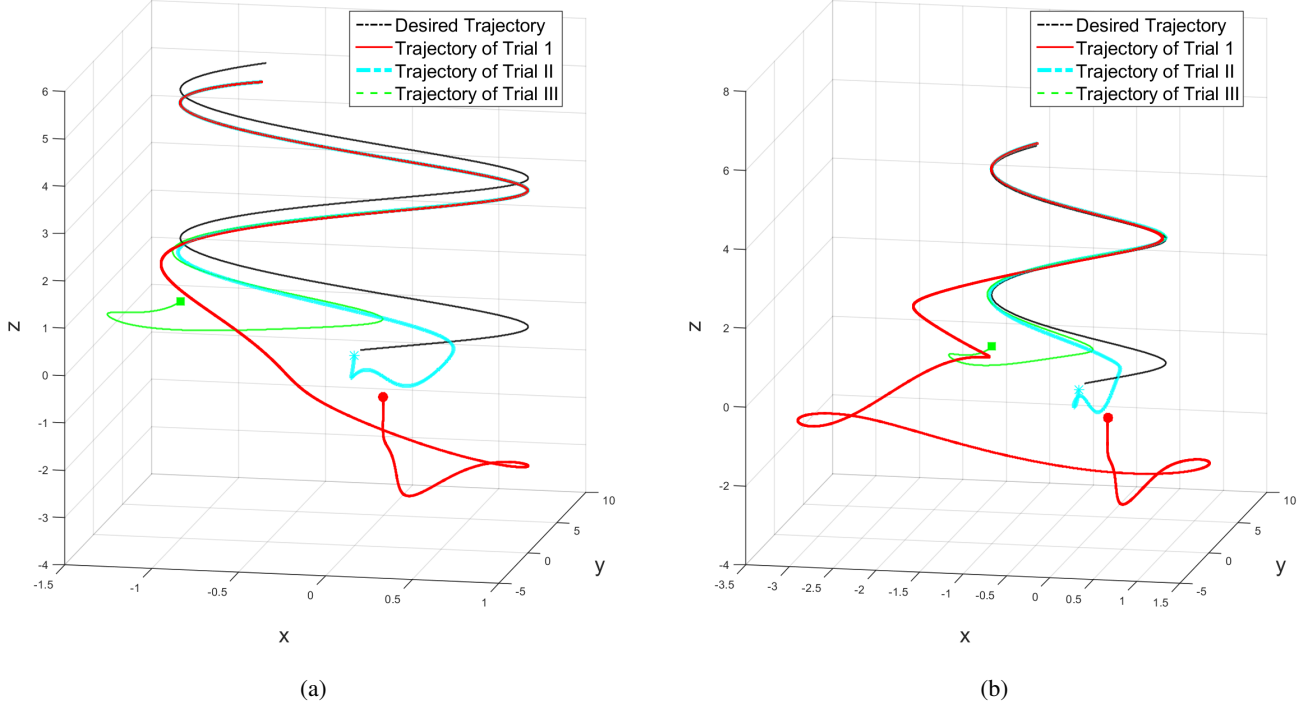


Fig. 7: Robustness results of the proposed controller for the quadrotor with a load system with model uncertainty. (a) The mass of the load is increased by 50%. Since the feedforward force is incorrect, asymptotic tracking is not realized. However, as can be seen, the trajectory for each trial remains close to the reference. This implies the boundedness of the error and thus robustness of this method. (b) The mass of the load is decreased by 10%. Here too we can see the boundedness of the error. However, as we continue to reduce the mass of the load further, Trial I becomes unstable and continues to drift away while Trials II and III still have bounded errors. Since Trial I starts with the quadrotor inverted, it's more sensitive to model uncertainty.

$$\begin{aligned}
\delta \dot{q} &= \delta \omega \times q_d + \omega_d \times \delta q, \\
m_Q L \delta \dot{\omega} &= -\delta q \times f_d R_d e_3 - \hat{q}_d (\delta f R_d e_3 + f_d \delta R e_3), \\
\delta \dot{R} &= R_d \delta \hat{\Omega} + \delta R \hat{\Omega}_d, \\
J_Q \delta \dot{\Omega} &= \delta M - \delta \Omega \times J_Q \Omega_d - \Omega_d \times J_Q \delta \Omega.
\end{aligned}$$

Rearranging each term, the error dynamics can be simplified into:

$$\begin{aligned}
\delta \dot{x}_L &= \delta v_L, \\
(m_Q + m_L) \delta \dot{v}_L &= [(q_d \cdot f_d R_d e_3 - m_Q L (\dot{q}_d \cdot \dot{q}_d)) I_3 \\
&\quad + q_d (f_d R_d e_3)^T] \delta q - 2m_Q L (q_d \dot{q}_d^T) \delta \dot{q} \\
&\quad + f_d \delta R e_3 + (q_d^T R_d e_3) \delta f, \\
\delta \dot{q} &= \hat{\omega}_d \delta q - \hat{q}_d \delta \omega, \\
m_Q L \delta \dot{\omega} &= \widehat{f_d R_d e_3} \delta q - \hat{q}_d f_d \delta R e_3 - \hat{q}_d R_d e_3 \delta f, \\
\delta \dot{R} &= R_d \delta \hat{\Omega} + \delta R \hat{\Omega}_d, \\
J_Q \delta \dot{\Omega} &= (\widehat{J_Q \Omega_d} - \hat{\Omega}_d J_Q) \delta \Omega + \delta M.
\end{aligned}$$

Now, reusing the conclusions already attained for the 3D pendulum and spherical pendulum, we can further simplify these equations to obtain,

$$\delta \dot{x}_L = \delta v_L,$$

$$\begin{aligned}
(m_Q + m_L) \delta \dot{v}_L &= -[(q_d \cdot f_d R_d e_3 - m_Q L (\dot{q}_d \cdot \dot{q}_d)) I_3 \\
&\quad + q_d (f_d R_d e_3)^T] \hat{q}_d \xi \\
&\quad - 2m_Q L q_d \dot{q}_d^T (-\hat{\omega}_d \hat{q}_d \xi - \hat{q}_d \delta \omega) \\
&\quad - f_d R_d \hat{e}_3 \eta + (q_d^T R_d e_3) \delta f, \\
\dot{\xi} &= q_d q_d^T (\omega_d \times \xi) + (I_3 - q_d q_d^T) \delta \omega, \\
m_Q L \delta \dot{\omega} &= -\widehat{f_d R_d e_3} \hat{q}_d \xi + \hat{q}_d f_d R_d \hat{e}_3 \eta - \hat{q}_d R_d e_3 \delta f, \\
\dot{\eta} &= -\hat{\Omega}_d \eta + I_3 \delta \Omega, \\
J_Q \delta \dot{\Omega} &= (\widehat{J_Q \Omega_d} - \hat{\Omega}_d J_Q) \delta \Omega + \delta M.
\end{aligned}$$

Also, using the vector triple product and the fact that $\omega_d \cdot q_d = 0$, we have,

$$\hat{\omega}_d \hat{q}_d \xi = (\xi \cdot \omega_d) q_d - (\omega_d \cdot q_d) \xi = (\xi \cdot \omega_d) q_d.$$

Right multiply the above equation by \hat{q}_d^T on both sides, and recognizing that $q_d \cdot \dot{q}_d = 0$, we have,

$$\hat{q}_d^T \hat{\omega}_d \hat{q}_d \xi = \hat{q}_d^T q_d (\xi \cdot \omega_d) = (q_d \cdot \dot{q}_d) (\xi \cdot \omega_d) = 0.$$

We can then finally write down the linearized error dynamics for the quadrotor with a cable-suspended load as the following:

$$\delta \dot{x}_L = \delta v_L,$$

$$\begin{aligned}
(m_Q + m_L)\delta\dot{v}_L &= -\{[(q_d \cdot f_d R_d e_3 - m_Q L(\dot{q}_d \cdot \dot{q}_d))I_3 \\
&\quad + q_d(f_d R_d e_3)^T \hat{q}_d]\xi + (2m_Q L q_d \hat{q}_d^T \dot{q}_d)\delta\omega \\
&\quad - f_d R_d \hat{e}_3 \eta + (q_d^T R_d e_3)\delta f, \\
\dot{\xi} &= (q_d q_d^T \hat{\omega}_d)\xi + (I_3 - q_d q_d^T)\delta\omega, \\
m_Q L \delta\dot{\omega} &= -\widehat{f_d R_d e_3} \hat{q}_d \xi + \hat{q}_d f_d R_d \hat{e}_3 \eta - \hat{q}_d R_d e_3 \delta f, \\
\dot{\eta} &= -\widehat{\Omega}_d \eta + I_3 \delta\Omega, \\
J_Q \delta\dot{\Omega} &= (\widehat{J_Q \Omega}_d - \widehat{\Omega}_d J_Q)\delta\Omega + \delta M,
\end{aligned}$$

which is of the form (5)-(6), with the state $s = [\delta x_L \ \delta v_L \xi \ \delta\omega \ \eta \ \delta\Omega]^T$, and constraint $q_d \cdot \xi \equiv 0$. Recognizing that this constraint is equivalent to $q_d \cdot \xi = \frac{d}{dt}(q_d \cdot \xi) = 0$, we can write this in matrix form as $Cs = 0$, where

$$C = \begin{bmatrix} 0_{1 \times 6} & q_d^T & 0_{1 \times 3} & 0_{1 \times 6} \\ 0_{1 \times 6} & -\omega_d^T \hat{q}_d & q_d^T & 0_{1 \times 6} \end{bmatrix}.$$

REFERENCES

- [1] S. P. Bhat and D. S. Bernstein, "A topological obstruction to continuous global stabilization of rotational motion and the unwinding phenomenon," *Systems & Control Letters*, vol. 39, no. 1, pp. 63–70, January 2000.
- [2] P. Brunovsky, "A classification of linear controllable systems," *Kybernetika*, vol. 6, no. 3, pp. 173–188, 1970.
- [3] F. Bullo and A. D. Lewis, *Geometric Control of Mechanical Systems*. New York-Heidelberg-Berlin: Springer-Verlag, 2004.
- [4] N. A. Chaturvedi, A. K. Sanyal, and H. McClamroch, "Rigid-body attitude control," *IEEE Control Systems Magazine*, vol. 31, no. 3, pp. 30–51, June 2011.
- [5] Y. Duan, S. Patil, J. Schulman, K. Goldberg, and P. Abbeel, "Planning locally optimal, curvature-constrained trajectories in 3d using sequential convex optimization," in *Robotics and Automation (ICRA), 2014 IEEE International Conference on*. IEEE, 2014, pp. 5889–5895.
- [6] M. Fliess, J. Lévine, P. Martin, and P. Rouchon, "Flatness and defect of nonlinear systems: Introductory theory and examples," CAS, Internal Report A-284, January 1994.
- [7] F. Goodarzi, D. Lee, and T. Lee, "Geometric stabilization of quadrotor uav with a payload connected by flexible cable."
- [8] M. Green and D. J. N. Limebeer, *Linear Robust Control*. Dover Publications, 2012.
- [9] A. Ilchmann and M. Mueller, "Time-varying linear systems: Relative degree and normal form," *IEEE Transactions on Automatic Control*, vol. 52, no. 5, pp. 840–851, May 2007.
- [10] H. K. Khalil, *Nonlinear Systems*, 3rd ed. Prentice Hall, 2002.
- [11] M. Kobilarov, "Discrete optimal control on lie groups and applications to robotic vehicles," in *Robotics and Automation (ICRA), 2014 IEEE International Conference on*. IEEE, 2014, pp. 5523–5529.
- [12] T. Lee, "Robust global exponential attitude tracking controls on $so(3)$," in *IEEE American Control Conference*, June, 2013, pp. 2103–2108.
- [13] T. Lee, M. Leok, and N. McClamroch, "Lagrangian mechanics and variational integrator on two-spheres," *International Journal for Numerical Methods in Engineering*, vol. 79, pp. 1147–1174, March 2009.
- [14] —, "Stable manifolds of saddle equilibria for pendulum dynamics on s^2 and $so(3)$," in *IEEE Conference on Decision and Control and European Control Conference*, December 2011, pp. 3915–3921.
- [15] —, "Dynamics and control of a chain pendulum on a cart," in *IEEE Conference on Decision and Control*, 2012, pp. 2502–2508.
- [16] —, "Control of complex maneuvers for a quadrotor uav using geometric methods on $se(3)$," *Asian Journal of Control*, vol. 15, no. 3, pp. 1–18, 2013.
- [17] T. Lee, K. Sreenath, and V. Kumar, "Geometric control of cooperating multiple quadrotor UAVs with a suspended payload," in *IEEE Conference on Decision and Control (CDC)*, Florence, Italy, December 2013, pp. 5510–5515.
- [18] A. D. Lewis, "Linearisation of tautological control systems," *Submitted to J Geom Mech*, 2014.
- [19] D. Liberzon, *Calculus of Variations and Optimal Control Theory*, 1st ed. Princeton University Press, 2012.
- [20] J. Marsden and T. Ratiu, *Introduction to Mechanics and Symmetry*, 2nd ed. Springer Verlag Press, 2002.
- [21] J. Milnor, *Morse Theory*. Princeton: Princeton University Press, 1963.
- [22] G. Peichl and W. Schappacher, "Constrained controllability in banach spaces," *SIAM Journal on Control and Optimization*, vol. 24, no. 6, 1986.
- [23] A. Saccon, J. Hauser, and A. P. Aguiar, "Optimal control on lie groups: The projection operator approach," *IEEE Transactions on Automatic Control*, vol. 58, no. 9, pp. 2230–2245, September 2013.
- [24] A. Saccon, J. Trumppf, R. Mahony *et al.*, "Second-order-optimal filters on lie groups," in *Decision and Control (CDC), 2013 IEEE 52nd Annual Conference on*. IEEE, 2013, pp. 4434–4441.
- [25] S. Sastry, *Nonlinear Systems*. Springer Verlag Press, 1999.
- [26] J. Schulman, Y. Duan, J. Ho, A. Lee, I. Awwal, H. Bradlow, J. Pan, S. Patil, K. Goldberg, and P. Abbeel, "Motion planning with sequential convex optimization and convex collision checking," *The International Journal of Robotics Research*, vol. 33, no. 9, pp. 1251–1270, 2014.
- [27] M. D. Shuster, "A survey of attitude representations," *Journal of the Astronautical Sciences*, vol. 41, no. 4, pp. 439–517, December 1993.
- [28] E. D. Sontag, "Controllability and linelinar regulation," *IEEE Transactions on Automatic Control*, vol. 32, no. 10, pp. 877–888, October 1987.
- [29] M. W. Spong, "Partial feedback linearization of underactuated mechanical systems," in *Intelligent Robots and Systems '94. Advanced Robotic Systems and the Real World', IROS'94. Proceedings of the IEEE/RSJ/GI International Conference on*, vol. 1. IEEE, 1994, pp. 314–321.
- [30] K. Sreenath and V. Kumar, "Dynamics, control and planning for cooperative manipulation of payloads suspended by cables from multiple quadrotor robots," in *Robotics: Science and Systems (RSS)*, 2013.
- [31] K. Sreenath, T. Lee, and V. Kumar, "Geometric control and differential flatness of a quadrotor UAV with a cable-suspended load," in *IEEE Conference on Decision and Control (CDC)*, Florence, Italy, December 2013, pp. 2269–2274.
- [32] R. V. Til and W. E. Schmitendorf, "Constrained controllability of discrete-time systems with additive disturbances," in *IEEE Conference on Decision and Control*, Fort Lauderdale, FL, December 1985, pp. 874–875.
- [33] D. R. Tyner and A. D. Lewis, "Geometric jacobian linearization and lqr theory," *Journal of Geometric Mechanics*, vol. 2, no. 4, pp. 397–440, 2010.